J. Fluid Mech. (2012), *vol.* 695, *pp.* 467–477. © Cambridge University Press 2012
doi:10.1017/jfm.2012.38

On sloshing modes in a circular tank

Odd M. Faltinsen† and Alexander N. Timokha

Centre for Ships and Ocean Structures & Department of Marine Technology,
Norwegian University of Science and Technology, NO-7091 Trondheim, Norway

(Received 12 December 2011; revised 14 January 2012; accepted 17 January 2012;
first published online 16 February 2012)

Employing the multipole-type functions given by Faltinsen & Timokha (*J. Fluid Mech.*, vol. 665, 2010, pp. 457–479), we derive a Trefftz-type representation of the velocity potential for the liquid sloshing problem in a two-dimensional circular tank. This representation defines a continuation of the velocity potential into the 'air' area confined by the 'dry' tank surface. Its usage facilitates an effective approximation of the natural sloshing modes for all tank fillings.

Key words: interfacial flows (free surface)

1. Introduction

Sloshing must be considered for almost any moving vehicle or for structures containing a liquid with a free surface. Various applications can be found in Faltinsen & Timokha (2009, chap. 1) as well as in the book by Ibrahim (2005). The studied two-dimensional sloshing problem in a circular tank is associated with transverse waves in a horizontal cistern. Owing to the volume conservation condition, constructing an analytical approximate velocity potential for inviscid liquid sloshing problems requires an *exact* satisfaction of the Laplace equation and the wetted tank–surface condition (Faltinsen & Timokha 2009). Moreover, a weakly nonlinear solution requires an analytical continuation of the velocity potential above the mean free surface. Referring to experiments by Barkowiak, Gampert & Siekmann (1985), Faltinsen & Timokha (2010) proposed a Trefftz solution of the linear sloshing problem based on a special set of harmonic functions satisfying the zero-Neumann condition everywhere on the circular wall except in the highest point of the tank where these functions imply multipole-type behaviour. By using the Kelvin inversion, similar harmonic functions were recently constructed by Barnyak *et al.* (2011) for the spherical tank.

Unfortunately, employing these sets of functions did not provide an effective approximation of the natural sloshing modes for higher ratios of liquid depth to tank radius, $h/R_0 \geqslant 1$. A formal mathematical clarification comes from the specific local 'singular' asymptotic behaviour of natural sloshing modes at the contact line (points) of a flat mean free surface and a circular wall (see theorems by Wigley 1964, 1970; Komarenko 1980) that is not captured by the constructed harmonic functions. Faltinsen & Timokha (2010) used correcting functions that account for the behaviour and showed that this enables a more accurate approximation of the natural sloshing modes for higher liquid fillings. However, employing these correcting functions implies non-changing contact points and angles that have no physical meaning for the nonlinear

† Email address for correspondence: oddfal@marin.ntnu.no

https://doi.org/10.1017/jfm.2012.38 Published online by Cambridge University Press

sloshing problem. Therefore, the modified Trefftz solution cannot be adopted for the nonlinear sloshing problem. We need another analytical representation for the sloshing velocity potential that is applicable for higher tank fillings and has a clear mathematical and physical treatment for the linear and nonlinear cases. Such a representation is proposed in the present paper by considering the continuation of the velocity potential into the 'air' area.

To begin, we discuss the continuation of the Trefftz solution by Faltinsen & Timokha (2010) and emphasize its inconsistency from experimental and theoretical points of view (Barkowiak *et al.* 1985; Kuznetsov, Spector & Zakharov 1994). In § 2, we try to improve it by distributing tangential multipoles with singularities along the 'dry' tank surface. This deduces an integral representation of the velocity potential with strength functions possessing special properties at the ends of the 'dry' tank area (to provide the finiteness of the velocity field; Komarenko 1980). Requiring the representation to be uniformly valid for arbitrary liquid depths means continuously differentiable strength functions (up to a certain order) on the whole 'dry' tank surface *except* in the tank top. As a consequence, we derive a new Trefftz solution, which includes (i) the solution by Faltinsen & Timokha (2010), (ii) a modified Poisson integral depending on the fully continuous component of the strength functions, and (iii) terms that are proportional to the jumps of the strength functions at the tank top. Generally speaking, this new solution returns an analytical harmonic function in the *inner* points of the whole circular tank domain, i.e. both the velocity potential and its continuation are constructed. In § 3, we report numerical results based on the new Trefftz-type solution. The solution is uniformly accurate for arbitrary liquid depths and enables one to study the limiting case $h/R_0 \to 2$ associated with the ice-fishing problem.

2. Theory

2.1. *Preliminaries and statement of the problem*

According to Barkowiak *et al.* (1985), the first sloshing mode in a circular tank with the depth/radius ratio $h/R_0 < 1$ can be satisfactorily approximated by a horizontal dipole with singularity at the tank top. The function W_1 in figure 1(*a*) presents the corresponding dipole-type velocity potential and associated streamlines. Assuming that other sloshing modes can be considered as a superposition of similar multipole-type flows, Faltinsen & Timokha (2010) postulated the Trefftz solution for the velocity potential as the sum

$$\Phi(y, z) = \sum_{i=0}^{N} d_i W_i(y, z), \tag{2.1}$$

where the analytical harmonic functions

$$W_k(y, z) = \sum_{i=0}^{[k/2]} (-1)^i \binom{k}{2i} \left(\frac{2y}{y^2 + (z-1)^2}\right)^{k-2i} \times \left(-1 - \frac{2(z-1)}{y^2 + (z-1)^2}\right)^{2i}, \quad k \geqslant 0, \tag{2.2}$$

imply a set of multipoles with singularities in the tank top.

Statements of the linear sloshing problem can be found in diverse textbooks (e.g. Ibrahim 2005; Faltinsen & Timokha 2009). When $\phi(y, z, t)$ is the velocity potential

https://doi.org/10.1017/jfm.2012.38 Published online by Cambridge University Press

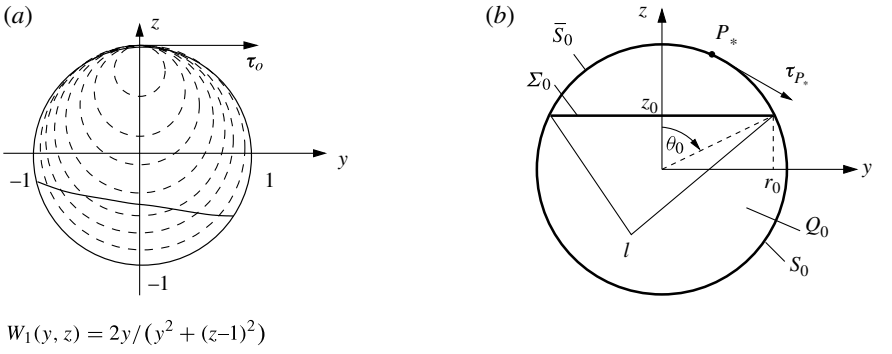


FIGURE 1. (*a*) The horizontal dipole harmonic function from the functional set by Faltinsen & Timokha (2010). The dashed lines denote the associated streamlines; $\boldsymbol{\tau}_O = (1, 0)$ is the tangential (horizontal) vector to the circle. (*b*) The geometric notation to the spectral boundary problem (2.3). A multipole can be posed at P_*, where $\boldsymbol{\tau}_{P_*}$ is the tangential vector.

and $z = \zeta(y, t)$ defines small-magnitude vertical displacements of the free surface, the free liquid oscillations deal with the zero-Neumann boundary condition for ϕ on the wetted tank surface S_0 as well as kinematic $\partial\phi/\partial z = \partial\zeta/\partial t$ and dynamic $\partial\phi/\partial t + g\zeta = 0$ boundary conditions on the mean free surface Σ_0 (g is the gravitational acceleration). The geometric notation for the two-dimensional transverse sloshing in a horizontal circular cylindrical tank is shown in figure 1(*b*) (non-dimensional case). For the natural sloshing problem, $\phi = \mathrm{i}\sigma \exp(\mathrm{i}\sigma t)\Phi(y, z)$, $\zeta = \exp(\mathrm{i}\sigma t)Z(y)$, $\mathrm{i}^2 = -1$, and one can recombine the boundary conditions on Σ_0 (see e.g. Faltinsen & Timokha 2009, chap. 4) to obtain the *non-dimensional* spectral boundary problem on the natural sloshing modes and frequencies

$$\boxed{\nabla^2\Phi = 0 \text{ in } Q_0; \quad \frac{\partial\Phi}{\partial n} = 0 \text{ on } S_0;} \quad \frac{\partial\Phi}{\partial z} = \kappa\Phi \text{ on } \Sigma_0; \quad \int_{\Sigma_0} \Phi \,\mathrm{d}S = 0, \tag{2.3}$$

where the natural sloshing frequencies are defined by $\sigma = \sqrt{\kappa g/R_0}$ (κ is the spectral parameter, and Φ are the natural sloshing modes).

The functions W_i are chosen to *exactly* satisfy the framed boundary conditions of (2.3) for arbitrary liquid depths. The Trefftz solution (2.1) satisfies the zero-Neumann condition not only on the wetted but also on the 'dry' tank surface $\bar{S}_0$ except in the upper tank pole. This may be a reason why this solution fails for higher liquid depths, $z_0 > 0$. To relax the zero-Neumann condition at a point $P_* \in \bar{S}_0$, one can 'rotate' the functions (2.2) around the circle centre so that the singularity can appear everywhere on the 'dry' tank surface. Our idea consists of integrating these singularities over $\bar{S}_0$ accompanied by a strength function. The result is an approximate velocity potential in the physical plane, which, generally, does not satisfy the zero-Neumann condition on $\bar{S}_0$ but leads to a zero-normal flow on S_0.

2.2. *Tangential multipoles with a single singularity*

Let $P = (y, z)$ (radius vector $\boldsymbol{P}$) be an arbitrary point in the Oyz-plane and $P_* = (y_*, z_*)$ be a point (radius vector $\boldsymbol{P}_*$) belonging to the 'dry' tank surface $\bar{S}_0$. The function

$$F_c(P; P_*) = \nabla_{(y,z)} G_c(P; P_*) \cdot \boldsymbol{\tau}_{P_*} = -\nabla_{(y_*,z_*)} G_c(P; P_*) \cdot \boldsymbol{\tau}_{P_*}, \tag{2.4}$$

https://doi.org/10.1017/jfm.2012.38 Published online by Cambridge University Press

$$G_c(P; P_*) = \ln|\,(y-y_*)^2 + (z-z_*)^2\,| \tag{2.5}$$

($\boldsymbol{\tau}_{P_*}$ is the tangential vector at P_* in the clockwise direction) is then a *generalization* of W_1. The function F_c implies now not horizontal but rather a *tangential dipole* at the point P_*. It satisfies the zero-Neumann condition everywhere on the circle, except at P_*. When $P_* = (0, 1)$, $\boldsymbol{\tau}_{P_*} = \boldsymbol{\tau}_O = (1, 0)$ and $W_1(y, z) = F_c(y, z; 0, 1)$.

We adopt the geometric notation in figure 1(*b*) with $P_* = (y_*, z_*) = (\sin\theta, \cos\theta)$, $-\theta_0 < \theta < \theta_0$ and $\boldsymbol{\tau}_{P_*} = \mathrm{d}P_*/\mathrm{d}\theta = (\cos\theta, -\sin\theta)$. As a consequence, the function G_c given by (2.4)–(2.5) transforms to the form

$$\mathscr{G}_c(y, z; \theta) = G_c(y, z; \sin\theta, \cos\theta) = \ln|\,(y-\sin\theta)^2 + (z-\cos\theta))^2|\,| \tag{2.6}$$

and we arrive at the following expression for the tangential dipole F_c:

$$\mathscr{F}_c(y, z; \theta) = F_c(y, z; \sin\theta, \cos\theta) = -\frac{\partial \mathscr{G}_c(y, z; \sin\theta, \cos\theta)}{\partial\theta}. \tag{2.7}$$

In the particular case, $W_1(y, z) = -\mathscr{F}_c(y, z; 0)$.

Furthermore, we can consider the kth derivative of $\mathscr{G}_c$ with respect to θ. All these derivatives keep the zero-Neumann condition on the circle except at the point $P_* = (\sin\theta, \cos\theta)$. The functions

$$\frac{\partial^{k-1}\mathscr{F}_c(y, z; \theta)}{\partial\theta^{k-1}} = -\frac{\partial^k \mathscr{G}_c(y, z; \sin\theta, \cos\theta)}{\partial\theta^k}, \quad k \geqslant 1, \tag{2.8}$$

define a special class of *tangential multipoles with a single singular point*, which satisfy the framed conditions of (2.3) as $-\theta_0 < \theta < \theta_0$. When $\theta = 0$, formula (2.8) gives a linear combination of W_i, namely,

$$\left.\frac{\partial \mathscr{G}_c}{\partial\theta}\right|_{\theta=0} = W_1(y, z); \quad \left.\frac{\partial^2 \mathscr{G}_c}{\partial\theta^2}\right|_{\theta=0} = \frac{1}{2}\,(W_2(y, z) + W_0(y, z))\,,$$
$$\left.\frac{\partial^3 \mathscr{G}_c}{\partial\theta^3}\right|_{\theta=0} = \frac{1}{2}\,(W_3(y, z) + W_1(y, z))\,,$$
$$\left.\frac{\partial^4 \mathscr{G}_c}{\partial\theta^4}\right|_{\theta=0} = \frac{3}{4}\left(W_4(y, z) + \frac{4}{3}W_2 + 3W_0(y, z)\right),$$
$$\left.\frac{\partial^5 \mathscr{G}_c}{\partial\theta^5}\right|_{\theta=0} = \frac{3}{2}\left(W_5(y, z) - \frac{10}{3}W_3(y, z) - 2W_1(y, z)\right), \quad \ldots.$$

2.3. *Integral representation of the velocity potential*

Varying $-\theta_0 < \theta < \theta_0$ in (2.8) and introducing the corresponding strength functions $w_k(\theta)$ for the tangentially situated multipoles, we can consider a resulting flow in the Oyz-plane by defining the velocity potentials

$$\phi_k(y, z) = \tilde{C} - \int_{-\theta_0}^{\theta_0} w_k(\theta)\,\frac{\partial^k \mathscr{G}_c}{\partial\theta^k}\,\mathrm{d}\theta, \quad k \geqslant 1. \tag{2.9}$$

The velocity potentials $\phi_k(y, z)$ satisfy the framed condition in (2.3), but, generally, do not satisfy the zero-Neumann boundary condition on $\bar{S}_0$. The features of the velocity potentials *strongly depend* on the strength functions $w_k(\theta)$, which can be non-continuous.

https://doi.org/10.1017/jfm.2012.38 Published online by Cambridge University Press

2.4. *The sloshing velocity potential*

When ϕ_k is the velocity potential associated with the sloshing problems, for example, Φ in (2.3), the corresponding velocity and pressure fields should remain finite in the vicinity of the free surface (here, Σ_0). We refer to Komarenko (1980), who proved the corresponding theorem for (2.3), as well as to certain physical arguments. This finiteness requires the strength function $w_k(\theta)$ to be k times continuously differentiable in a neighbourhood of $\pm\theta_0$ and, in addition, the local condition

$$w_k(\pm\theta_0) = \cdots = \frac{d^k w_k}{d\theta^k}(\pm\theta_0) = 0, \quad k \geqslant 1, \tag{2.10}$$

should be satisfied.

Our goal is a solution that is uniformly valid for arbitrary liquid, i.e. defining

$$w_k(\theta) = \begin{cases} w_k^-(\theta) & \text{for } -\theta_0 < \theta < 0, \\ w_k^+(\theta) & \text{for } 0 < \theta < \theta_0, \end{cases} \tag{2.11}$$

we require $w_k^\pm$ to be k *times continuously differentiable* on the potentially wetted tank surface, namely, on the two subintervals $[-\theta_0, 0)$ and $(0, \theta_0]$. The only *exception* is the point $\theta = 0$, which is not reachable by liquid for non-empty Σ_0, so that a jump between $w_k^\pm$ and their derivatives at $\theta = 0$ is possible. Considering a linear combination of ϕ_k, $k = 1, \ldots, N+1$, with (2.11) and using recursive integration by parts on $(-\theta_0, 0)$ and $(0, \theta_0)$ leads to the expression

$$\begin{aligned} \Phi(y,z) = C + \sum_{i=1}^{N} d_i \frac{\partial^i \mathscr{G}_c}{\partial\theta^i} + \left(\mathscr{W}^+(0) - \mathscr{W}^-(0)\right)\mathscr{G}_c(y,z;0) \\ + \int_{-\theta_0}^{0} \frac{\mathrm{d}\mathscr{W}^-}{\mathrm{d}\theta}\mathscr{G}_c(y,z;\theta)\,\mathrm{d}\theta + \int_{0}^{\theta_0} \frac{\mathrm{d}\mathscr{W}^+}{\mathrm{d}\theta}\mathscr{G}_c(y,z;\theta)\,\mathrm{d}\theta, \end{aligned} \tag{2.12}$$

with

$$\mathscr{W}(\theta) = \begin{cases} \mathscr{W}^-(\theta) & \text{for } -\theta_0 < \theta < 0, \\ \mathscr{W}^+(\theta) & \text{for } 0 < \theta < \theta_0, \end{cases} \quad \text{and} \quad \mathscr{W}^\pm(\pm\theta_0) = (\mathscr{W}^\pm)'(\pm\theta_0) = 0, \tag{2.13}$$

where $\mathscr{W}^\pm(\theta)$ is a rather complicated linear combination of $w_k^\pm$ and their derivatives (C is a combination of earlier $\tilde{C}$). The exact expression for $\mathscr{W}^\pm$ does not play a role in the forthcoming analysis, so that we can start by considering (2.12) with two arbitrary continuously differentiable functions $\mathscr{W}^\pm(\theta)$ on subintervals $(-\theta_0, 0)$ and $(0, \theta_0)$.

After introducing an auxiliary analytical 'density' function satisfying the conditions

$$\begin{cases} \rho_w(\pm\theta_0) = \rho_w'(\pm\theta_0) = 0, \quad \rho_w(\theta) > 0, \quad -\theta_0 < \theta < \theta_0, \\ \rho_w(0) = 1, \quad \rho_w'(0) = 0, \end{cases} \tag{2.14}$$

formula (2.12) can be rewritten by introducing the continuously differentiable component $\mathscr{W}_c(\theta)$ of the strength function on $[-\theta_0, \theta_0]$ using the formula

$$\mathscr{W}(\theta) = \tfrac{1}{2}\rho_w(\theta)[(\mathscr{W}^+(0) - \mathscr{W}^-(0))\,\mathrm{sgn}(\theta) + ((\mathscr{W}^+)'(0) - (\mathscr{W}^-)'(0))\,|\theta|] + \mathscr{W}_c(\theta). \tag{2.15}$$

https://doi.org/10.1017/jfm.2012.38 Published online by Cambridge University Press

With definitions (2.15) and (2.14), formula (2.12) reduces to

$$\Phi(y,z) = C + \sum_{i=1}^{N} d_i \frac{\partial^i \mathscr{G}_c}{\partial \theta^i} + \underbrace{\tfrac{1}{2}(\mathscr{W}^+(0) - \mathscr{W}^-(0))}_{c_0^{(1)}} \times \underbrace{\left[2\mathscr{G}_c(y,z;0) - \int_{-\theta_0}^{0} \rho_w' \mathscr{G}_c \,\mathrm{d}\theta + \int_{0}^{\theta_0} \rho_w' \mathscr{G}_c \,\mathrm{d}\theta\right]}_{F_c(y,z;\rho_w)} + \underbrace{\tfrac{1}{2}\left((\mathscr{W}^+)'(0) - (\mathscr{W}^-)'(0)\right)}_{c_0^{(2)}} \times \underbrace{\left[-\int_{-\theta_0}^{0} (\theta\rho_w'(\theta) + \rho_w)\mathscr{G}_c \,\mathrm{d}\theta + \int_{0}^{\theta_0} (\theta\rho_w'(\theta) + \rho_w)\mathscr{G}_c \,\mathrm{d}\theta\right]}_{F_d(y,z;\rho_w)} + \int_{-\theta_0}^{\theta_0} \frac{\mathrm{d}\mathscr{W}_c}{\mathrm{d}\theta} \mathscr{G}_c(y,z;\theta)\,\mathrm{d}\theta. \tag{2.16}$$

We see that our representation of the velocity potential (2.16) contains three different components. First, because $\partial^i \mathscr{G}_c/\partial\theta^i$ is a finite linear combination of $W_i(y,z)$, the first sum in (2.12) is the *same* as the Trefftz solution by Faltinsen & Timokha (2010). It implies a discrete strength distribution in the upper tank pole. Secondly, the last integral is the same as the modified Poisson integral for the Neumann boundary problem in the circle (Polyanin 2001, §§ 7.1.2–3) returning an analytical harmonic function in the whole circle for the continuous (here, artificial) normal velocity on $\bar{S}_0 \cup S_0$:

$$v_n(\theta) = -\frac{1}{2\pi}\mathscr{W}_c'(\theta), \quad -\theta_0 < \theta < \theta_0 \quad \text{and} \quad v_n(\theta) = 0 \quad \text{on } S_0. \tag{2.17}$$

Equation (2.13) provides the solvability condition $\int_{-\pi}^{\pi} v_n \,\mathrm{d}\theta = 0$ for this modified Poisson integral. The integral implies a continuous strength distribution component along the 'dry' tank surface. Thirdly, the formula (2.16) also includes a linear combination of the two harmonic functions, F_d and F_c, which implies both discrete strength distribution associated with jumps at $\theta = 0$ and a continuous strength component related to ρ_w. These two functions yield a log-type (source) singularity in the tank top point with the integrated source strength equal to zero.

3. Numerical results for the natural sloshing modes

3.1. *Variational Trefftz scheme*

We can approximate the function $\mathscr{W}_c$ by the sum $\mathscr{W}_c(\theta) = \sum_{k=1}^{q} \alpha_k b_k(\theta)$ $(q \to \infty)$ with unknown coefficients $\{\alpha_k\}$ and a complete set of continuously differentiable functions $b_k(\theta)$ satisfying the end conditions

$$b_k(\pm\theta_0) = b_k'(\pm\theta_0) = 0. \tag{3.1}$$

The natural sloshing modes in the circular tank fall into symmetric (even) and antisymmetric (odd) cases. Using the formula (2.16) for approximating the odd (antisymmetric) natural sloshing modes, Φ_{2j-1}, requires the symmetric (even) function

https://doi.org/10.1017/jfm.2012.38 Published online by Cambridge University Press

$\mathscr{W}_c$, $\mathscr{W}^+(0) = \mathscr{W}^-(0)$, and $d_{2i} = 0$. The symmetric (even) modes, Φ_{2j}, appear for the antisymmetric (odd) function $\mathscr{W}_c$, $(\mathscr{W}^+)'(0) = (\mathscr{W}^-)'(0)$, and $d_{2i-1} = 0$. Taking arbitrary constants C, d_i and $c_0^{(j)}$, we can write the natural sloshing modes as

$$\Phi_{2j-1}(y, z) = \sum_{i=1}^{N/2} d_{2i-1} \frac{\partial^{2i-1}\mathscr{G}_c}{\partial\theta^{2i-1}}(y, z) + c_0^{(2)} F_d(y, z) + \sum_{k=1}^{q} \alpha_k^{(2)} u_k(y, z), \tag{3.2a}$$

$$\Phi_{2j}(y, z) = C + \sum_{i=1}^{N/2} d_{2i} \frac{\partial^{2i}\mathscr{G}_c}{\partial\theta^{2i}}(y, z) + c_0^{(1)} F_c(y, z) + \sum_{k=1}^{q} \alpha_k^{(1)} u_k(y, z), \tag{3.2b}$$

where

$$u_k(y, z) = \int_{-\theta_0}^{\theta} \mathscr{G}_c(y, z; \theta) b_k'(\theta)\, \mathrm{d}\theta. \tag{3.3}$$

Each of the (y, z) functions in (3.2) satisfies the framed conditions in (2.3). Our task consists of finding the unknown coefficients C, d_i, $c_0^{(j)}$ and $\alpha_k^{(j)}$ by using a variational scheme to satisfy the spectral boundary condition on Σ_0 (see details in Faltinsen & Timokha 2010).

3.2. *Numerical experiments*

We conducted numerical experiments with the Trefftz solution (3.2) using different base functions $b_k(\theta)$ and $\rho_w(\theta) = (1 - (\theta/\theta_0)^2)^2$. The best convergence is established when $b_k(\theta)$ are similar to the Euler beam eigenmodes with the clamped ends defined on the intervals $[-\theta_0, 0]$ and $[0, \theta_0]$. These eigenmodes provide the end condition (3.1) as well as guaranteeing the continuity of the function $\mathscr{W}_c$ and its first derivative at $\theta = 0$. Convergence with other complete systems of functions, e.g. of trigonometric type, was also satisfactory. Our computations involve integrands with singularities at the ends and in the middle of $[-\theta_0, \theta_0]$. To handle these singularities, the Kress quadrature rules (see Kress 1990; Timokha 2005) were used. The Trefftz method showed a rapid convergence, so that the number $M = N/2 + 2 + q$ in the range between 8 and 20 normally provided stabilization of six–eight significant figures for 20 approximate natural eigenvalues κ_i and tested liquid depths ($0 < h/R_0 \leqslant 1.99995$). This number of significant figures is also consistent with the double-precision specifications in our non-optimized FORTRAN code, accuracy of the quadrature rules and the solver of the spectral matrix problem. The numerical eigenvalues fully agree with the particular cases by McIver (1989). Table 1 focuses on numerical results for higher liquid depths where the Trefftz solution by Faltinsen & Timokha (2010) failed.

A rapid convergence to the natural sloshing modes Φ_i was also established. Because these modes are defined to within a multiplier, the normalization $\int_{-r_0}^{r_0} |\Phi_i(y, z_0)|^2\, \mathrm{d}y = 1$, $i \geqslant 1$ was used. In the cases when the six–eight significant figures of the studied natural eigenvalues κ_i were stabilized, the method normally provided three–five significant figures of $\Phi(x, z_0)$ in the uniform metrics. Within the above normalization, the error $\epsilon_i = \sqrt{\int_{\Sigma_0} (\partial\Phi_i/\partial z - \bar{\kappa}_i\Phi_i)^2\, \mathrm{d}S}$ was established to be in the range between 10^{-3} and 10^{-7}.

To get a stable convergence, the lower tank fillings required lower q and larger N, but the higher tank fillings normally needed the number N to be between 0 and 3 and the larger number q. This implicitly indicates that the discrete, single-located multipole component in the tank top following from the paper by Faltinsen & Timokha

https://doi.org/10.1017/jfm.2012.38 Published online by Cambridge University Press

h/R_0	r_0	κ_1	κ_3	κ_5	κ_7	κ_9	κ_{11}
1.0	1.0	1.35573	4.65105	7.81986	10.9718	14.1189	17.2771
1.2	0.979796	1.50751	4.85091	8.07834	11.2932	14.5041	17.7132
1.4	0.84	1.73463	5.27678	8.72206	12.1571	15.5888	19.0190
1.6	0.8	2.12372	6.13932	10.0807	14.0138	17.9442	21.8734
1.8	0.6	3.02140	8.31389	13.5596	18.7997	24.0382	29.2758
1.9	0.435890	4.31118	11.5485	18.7600	25.9691	33.1776	40.3857
1.92	0.391918	4.83420	12.8716	20.8898	28.9066	36.9232	44.9398
1.94	0.341174	5.60256	14.8207	24.0282	33.2360	42.4440	51.6523
1.96	0.28	6.89493	18.1072	29.3219	40.5394	51.7582	62.9778
1.98	0.198997	9.82040	25.5633	41.3345	57.1141	72.8972	88.6819
1.99	0.141067	13.9661	36.1432	58.3829	80.6387	102.900	125.165
1.999	0.044710	44.6236	114.448	184.572	254.748	308.112	325.188
1.9999	0.014142	141.503	362.194	583.761	805.936	1027.54	1143.69
1.99995	0.009999	200.420	512.488	824.782	1138.13	1454.04	1769.45
		$r_0\kappa_1$	$r_0\kappa_3$	$r_0\kappa_5$	$r_0\kappa_7$	$r_0\kappa_9$	$r_0\kappa_{11}$
1.99995	0.009999	2.00418	5.12482	8.24772	11.38118	14.54030	17.6943
		Ice-fishing limit (Miles 1972; McIver 1989)					
2.0		2.00612	5.12530	8.25885	11.39820		

h/R_0	r_0	κ_2	κ_4	κ_6	κ_8	κ_{10}	κ_{12}
1.0	1.0	3.03310	6.23920	9.39668	12.5457	15.6955	19.0563
1.2	0.979796	3.21640	6.46747	9.68640	12.8988	16.1088	19.3187
1.4	0.84	3.53751	6.99993	10.4388	13.8722	17.3033	20.7333
1.6	0.8	4.14328	8.10314	12.0419	15.9749	19.9056	23.8351
1.8	0.6	5.62694	10.9061	16.1586	21.4033	26.6447	31.8843
1.9	0.435890	7.81443	15.0852	22.3173	29.5378	36.7534	43.9664
1.92	0.391918	8.70757	16.7955	24.8398	32.8709	40.8965	48.9190
1.94	0.341174	10.0226	19.3154	28.5571	37.7833	47.0029	56.2189
1.96	0.28	12.2388	23.5651	34.8274	46.0705	57.3051	68.5354
1.98	0.198997	17.2647	33.2070	49.0564	64.8775	80.6860	96.4882
1.99	0.141067	24.3946	46.8896	69.2504	91.5700	113.872	136.164
1.999	0.044710	77.1585	148.164	218.733	289.166	359.538	429.881
1.9999	0.014142	243.977	468.626	691.761	914.655	1137.26	1359.26
1.99995	0.009999	345.061	663.781	975.868	1293.61	1610.00	1923.44
		$r_0\kappa_2$	$r_0\kappa_4$	$r_0\kappa_6$	$r_0\kappa_8$	$r_0\kappa_10$	$r_0\kappa_{12}$
1.99995	0.009999	3.45057	6.637733	9.75856	12.9359	16.0998	19.23420
		Ice-fishing limit (Miles 1972; McIver 1989)					
2.0		3.45333	6.62861	9.78393	12.9330		

TABLE 1. The eigenvalues for antisymmetric κ_{2k-1} and symmetric κ_{2k} computed for higher liquid depths. When they exist, the numerical values fully agree with McIver (1989) and Faltinsen & Timokha (2010). The calculations show that the method enables a numerical handling of the asymptotic limit $h/R_0 \to 2$ when $r_0\kappa_i$ tends to the eigenvalues of the so-called ice-fishing problem.

(2010) gives a dominant contribution for lower tank fillings with $-1 < z_0 \lesssim 0$, but the opposite limit, $0.9 \lesssim z_0 < 1$, is characterized by the leading continuous strength function component $\mathscr{W}_c$. For the range $0 \lesssim z_0 \lesssim 0.9$, both discrete and continuous

https://doi.org/10.1017/jfm.2012.38 Published online by Cambridge University Press

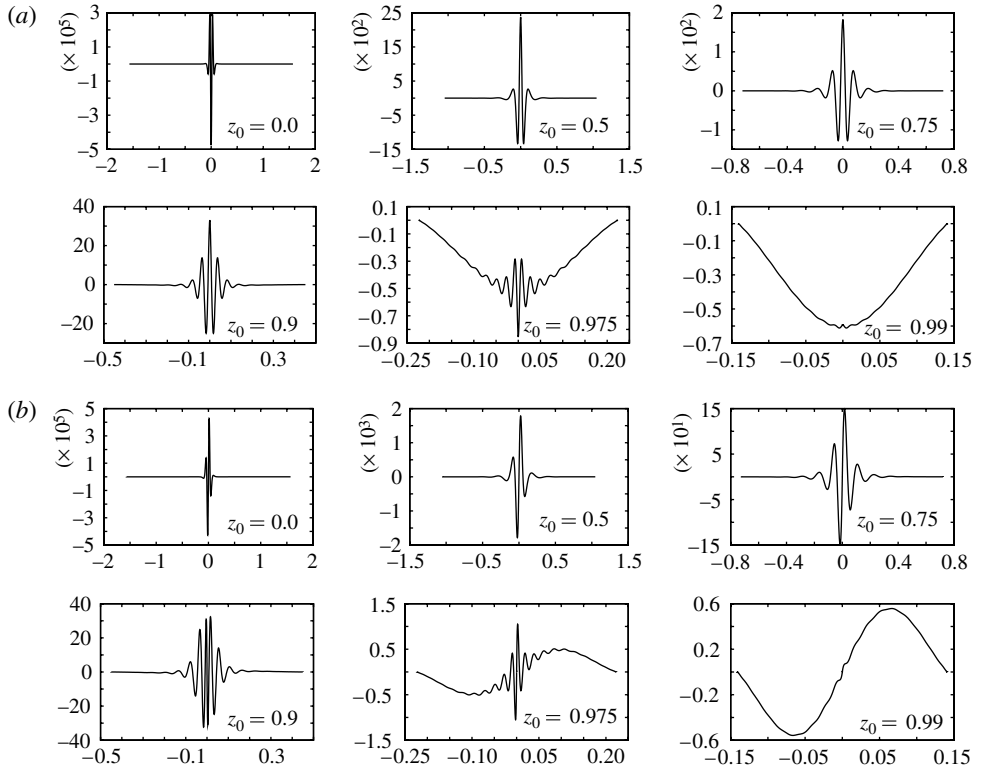


FIGURE 2. The strength function in (3.4) versus $z_0 = h/R_0 - 1$ for the first (a) antisymmetric and (b) symmetric modes. A passage to a purely continuous strength distribution as $z_0 \to 1$ is demonstrated. The computations were done with $\tau = 0.05$ in the approximation (3.4). The peak values of $\mathscr{W}_{c\tau}(\theta)$ can significantly change when varying τ with $-1 < z_0 \lesssim 0.975$.

strength function components matter. Even though our code does not have special normalization accounting for vanishing of the non-dimensional free surface length $2r_0 = 2\sqrt{1 - z_0^2}$, we tried to study numerically the natural sloshing modes and frequencies for the limiting case $h/R_0 \to 2$. Table 1 reports some results for the eigenvalues κ_i. The calculations remain stable up to $z_0 = 0.999\,99$. A control of the numerical eigenvalues for this limit can be done by recalling that the eigenvalues $r_0\kappa_i$ should tend to the eigenvalues for the so-called ice-fishing problem. The numerical limit values of the latter problem were presented, for example, by Miles (1972) and McIver (1989). Table 1 compares these numerical limiting values with our calculations done with $z_0 = 0.999\,95$. It looks like κ_i rapidly increases as z_0 is close to 1, but this is because the growth is proportional to $1/r_0$ with $r_0 = \sqrt{1 - z_0^2}$.

3.3. *Discrete versus continuous components of the strength function*

Even though the method demonstrates a rapid convergence to the natural modes and frequencies associated with the liquid domain Q_0, we were not able to establish the convergence for the continuous strength function $\mathscr{W}_c$ and the coefficients d_i and $c_0^{(j)}$ in formulae (3.2). Why is this so? First, we should remember that, even though the basic functions $\partial^i \mathscr{G}_c/\partial\theta^i$, F_c and F_d are infinite on the interval $(-\theta_0, \theta_0)$, the Trefftz solution in Q_0, being, in particular, defined by integral expressions involving these functions, is

https://doi.org/10.1017/jfm.2012.38 Published online by Cambridge University Press

finite together with the first derivatives. As a consequence, a small error in coefficients d_i and $c_0^{(j)}$ causes a small change for the natural sloshing modes and frequencies in Q_0, but may cause significant changes in $\mathscr{W}_c$ on $\bar{S}_0$ (first of all, at $\theta = 0$), which tries to 'compensate' the error in d_i and $c_0^{(j)}$ for obtaining the same liquid sloshing solution in Q_0, outside of $\bar{S}_0$.

A way to get information on a summarized strength function for different liquid depths may, for example, be a continuous approximation of d_i and $c_0^{(j)}$ related components by recalling that $\delta(\theta) = \lim_{\tau\to 0+}\delta_\tau(\theta) = \lim_{\tau\to 0+}\pi^{-1}\tau/(\tau^2+\theta^2)$ and the analogous τ approximations $\mathrm{sgn}_\tau(\theta) = \pi^{-1}\arctan(\theta/\tau)$ and $|\theta|_\tau = \pi^{-1}(\theta\arctan(\theta/\tau) - (\tau/2)\ln(1+(\theta/\tau)^2))$. Based on that, we can omit the discrete components in formula (2.15) by considering the only τ-dependent continuous strength function defined by

$$\mathscr{W}(\theta) = \mathscr{W}_c(\theta) := \mathscr{W}_{c\tau}(\theta) = \rho_w(\theta)\left[\sum_{i=1}^{N}(-1)^i d_i\,(\delta_\tau)^{(i-1)}(\theta) + c_0^{(1)}\frac{1}{\pi}\arctan\left(\frac{\theta}{\tau}\right)\right.$$
$$\left. + c_0^{(2)}\frac{1}{\pi}\left(\theta\arctan\left(\frac{\theta}{\tau}\right) - \frac{1}{2}\tau\ln\left(1+\left(\frac{\theta}{\tau}\right)^2\right)\right)\right] + \sum_{k=1}^{q}\alpha_k b_k(\theta). \qquad (3.4)$$

In the limit $\tau \to 0+$, the formula will transform to (2.15).

Using (3.4) with a fixed τ provides the convergence to the natural sloshing modes and frequencies. In addition, it demonstrates a convergence to the strength function $\mathscr{W}_{c\tau}$. A typical behaviour of $\mathscr{W}_{c\tau}$ for the first antisymmetric and symmetric modes computed with $\tau = 0.05$ is illustrated in figure 2. A small change of τ may significantly change the peak values about $\theta = 0$, but qualitatively function $\mathscr{W}_{c\tau}$ remains similar to those in figure 2.

4. Conclusions

We assumed that the continuation of the velocity potential yields an artificial multipole-type flow on the 'dry' tank surface $\bar{S}_0$ and, thereby, derived a new Trefftz solution that provides the zero-Neumann condition on the wetted tank surface. The solution contains the earlier solution by Faltinsen & Timokha (2010) and two new components associated with a continuous distribution of the artificial flows on $\bar{S}_0$. The solution was used to approximate the natural sloshing modes. Calculations confirmed that the solution remains accurate for both lower and higher tank fillings and, moreover, can be used for a numerical study of the limiting case of the completely filled tank. Studying the strength function on the 'dry' tank surface shows that the earlier solution component by Faltinsen & Timokha (2010) gives a dominant contribution for lower liquid depths, $0 < h/R_0 \lesssim 1$, and disappears for higher tank filling, $1.9 \lesssim h/R_0 < 2$, where the continuous strength contribution dominates. For $1 \lesssim h/R_0 \lesssim 1.9$, all the solution components give an equal contribution to the velocity potential.

The present approach can easily be generalized to the arbitrary two-dimensional sloshing problem for a smooth closed tank surface by using conformal mapping. Another point is that the sum in (3.2) gives the velocity potential of the nonlinear sloshing problem provided by C, the coefficients d_i, c_0^j and α_k^j are time-dependent functions and the integration in (3.3) is from $\theta_-(t)$ to $\theta_+(t)$ (associated with the contact points) and the analogous integration limits are given in the definitions of F_c and F_d. As required in the nonlinear multimodal method, this velocity potential satisfies the tank–surface condition and the newly introduced time-dependent functions can

https://doi.org/10.1017/jfm.2012.38 Published online by Cambridge University Press

be found from the kinematic and dynamic boundary conditions or the corresponding variational formulation.

REFERENCES

BARKOWIAK, K., GAMPERT, B. & SIEKMANN, J. 1985 On liquid motion in a circular cylinder with horizontal axis. *Acta Mechanica* **54**, 207–220.

BARNYAK, M., GAVRILYUK, I., HERMANN, M. & TIMOKHA, A. 2011 Analytical velocity potentials in cells with a rigid spherical wall. *Z. Angew. Math. Mech.* **91** (1), 38–45.

FALTINSEN, O. M. & TIMOKHA, A. N. 2009 *Sloshing*. Cambridge University Press.

FALTINSEN, O. M. & TIMOKHA, A. N. 2010 A multimodal method for liquid sloshing in a two-dimensional circular tank. *J. Fluid Mech.* **665**, 457–479.

IBRAHIM, R. 2005 *Liquid Sloshing Dynamics*. Cambridge University Press.

KOMARENKO, A. 1980 Asymptotic expansion of eigenfunctions of a problem with a parameter in the boundary conditions in a neighbourhood of angular boundary points. *Ukr. Math. J.* **32** (5), 433–437.

KRESS, R. 1990 A Nyström method for boundary integral equations in domains with corners. *Numer. Math.* **58**, 145–161.

KUZNETSOV, E. A., SPECTOR, M. D. & ZAKHAROV, V. E. 1994 Formation of singularities on the free surface of an ideal fluid. *Phys. Rev.* E **49**, 1283–1290.

MCIVER, P. 1989 Sloshing frequencies for cylindrical and spherical containers filled to an arbitrary depth. *J. Fluid Mech.* **201**, 243–257.

MILES, J. W. 1972 On the eigenvalue problem for fluid sloshing in a half-space. *Z. Angew. Math. Mech.* **23**, 861–869.

POLYANIN, A. D. 2001 *Handbook of Linear Partial Differential Equations for Engineers and Scientists*. Chapman and Hall/CRC.

TIMOKHA, A. N. 2005 Planimetry of vibrocapillary equilibria at small wavenumbers. *Intl. J. Fluid Mech. Res.* **32** (4), 454–487.

WIGLEY, N. M. 1964 Asymptotic expansions at a corner of solutions of mixed boundary value problems (asymptotic expansions at corner of solutions of elliptic second order partial differential equations in two variables). *J. Math. Mech.* **13**, 549–576.

WIGLEY, N. M. 1970 Mixed boundary value problems in plane domains with corners. *Math. Z.* **115**, 33–52.

https://doi.org/10.1017/jfm.2012.38 Published online by Cambridge University Press